Has Coarse Ocean Resolution Biased Simulations of Transient Climate Sensitivity?

Michael Winton, Whit G. Anderson, Thomas L. Delworth,
Stephen M. Griffies, William J. Hurlin and Anthony Rosati

Geophysical Fluid Dynamics Laboratory/NOAA, Princeton, New Jersey

Submitted to *Geophysical Research Letters*

28 October 2014

Corresponding author address: Michael Winton, NOAA/GFDL, Princeton University Forrestal Campus, 201 Forrestal Rd., Princeton, NJ 08540.
E-mail: Michael.Winton@noaa.gov

Abstract

We investigate the influence of ocean component resolution on simulation of climate sensitivity using variants of the GFDL CM2.5 climate model incorporating eddy-resolving ($1/10^{o}$) and eddy-parameterizing (1°) ocean resolutions. Two parameterization configurations of the coarse-resolution model are used yielding a three-model suite with significant variation in the transient climate response (TCR). The variation of TCR in this suite and in an enhanced group of 10 GFDL models is found to be strongly associated with the control climate Atlantic meridional overturning circulation (AMOC) magnitude and its decline under forcing. We find it is the AMOC behavior rather than resolution per se that accounts for most of the TCR differences. A smaller difference in TCR stems from the eddy-resolving model having more Southern Ocean surface warming than the coarse models.

1. Introduction

The scale of jet-like flows and transient eddies in the ocean is much smaller than that of the comparable features in the atmosphere. Consequently, these features have been resolved by the atmosphere components of climate models for decades but are only recently becoming resolved by the ocean components. Transient eddies are thought to be important to the simulation of both the ocean climate and its response to radiative forcing (e.g. Palter et al 2013) and so are represented by parameterizations. Uncertainty in the formulation and parameter values of the coarse resolution eddy parameterization introduces uncertainty into the transient response to radiative forcing (Kuhlbrodt and Gregory 2012). Recent increases in computer power have allowed for limited simulation with climate models employing ocean components with $1/10^{o}$ resolution (Kirtman et al 2011; McClean et al 2011; Delworth et al 2012; Bryan et al 2013). At $1/10^{o}$ resolution, these simulations can develop levels of eddy kinetic energy comparable to satellite estimates (Delworth et al 2012) allowing credible assessment of the role of eddy processes in climate change.

Here we diagnose the difference that eddy resolution makes to the simulation of transient climate sensitivity in the GFDL CM2.5 class climate models by comparing $1/10^{o}$ and 1° ocean resolutions coupled to the same 50 km atmosphere component. This comparison assesses possible biases in the projections that have been made to date using coarse resolution ocean components. The transient sensitivity is quantified with the transient climate response (TCR) the global surface warming at CO_2 doubling in a 1%/year CO2 increase experiment.

Similar resolution comparisons have been performed previously by Yokohata et al (2007) using two resolutions of the MIROC3.2 climate model, by Delworth et al (2012) comparing the transient sensitivity of GFDL's CM2.1 and CM2.5 climate models, and by Bryan et al (2013) using 1°- and $1/10^o$-ocean versions of the NCAR CCSM3.5 model. Yokohata et al (2007) found that the transient climate response for the higher resolution version of MIROC3.2, using a ¼ ^{o} ocean component, was 0.5 K higher than that using a lower resolution (1°) ocean – larger than the increase in equilibrium climate sensitivity (ECS) of 0.3 K – indicating a role for ocean resolution in the increased sensitivity. Delworth et al (2012) found, similarly, that CM2.5, employing a $1/4^o$ ocean had a TCR about 0.4 K larger than CM2.1 using a 1° ocean. The ECS for CM2.5 was not evaluated in that study. These two comparisons involved changes in atmospheric resolution as well as ocean resolution while the Bryan et al (2014) study with NCAR's CCSM3.5 made use of the same atmosphere coupled to both 1° and $1/10^o$ ocean components. They found that the TCR was unchanged by the resolution increase. Conventionally the ECS, the steady-state global warming induced by doubled CO_2, is assumed to be a property of the atmosphere and so it is assumed to be the same for both CCSM3.5 configurations.

Here we extend the Delworth et al (2012) investigation by employing $1/10^o$ and two 1° versions of the CM2.5 model coupling in the same atmosphere and land components and following the same spin up and CO_2 increase protocols for the three models. To evaluate the generality of our results, we enhance our three model suite with seven other previously published GFDL climate models. The models and experiments are described in the next section. Section three presents the results and section four discusses the conclusions.

2. Models and experiments

The models and experiments used in this study are summarized in Table S1. The ancestor model for the models used here is CM2.5 which employs a 1/4° ocean component and was described in detail by Delworth et al (2012). A short run of the 1/10° version of CM2.5, CM2.6, was also presented in that study showing that the eddy kinetic energy was increased over that of CM2.5 into agreement with a satellite estimate. CM2.6 does not make use of Gent-McWilliams eddy parameterization (Gent and McWilliams 1990) or background vertical mixing. We use two 1° versions of CM2.5, labeled "FLOR" for "Forecast Low Ocean Resolution", that require these parameterizations. Both of these coarse models have been used as part of the GFDL seasonal prediction system (Vecchi et al 2014). The use of two coarse models allows us to span a primary tuning uncertainty that determines the model Atlantic meridional overturning circulation (AMOC) magnitude. The magnitude of the AMOC is related to the magnitude of its decline (Gregory et al 2005) and consequently has a major impact on the transient response at high latitudes in the Northern Hemisphere (Rugenstein et al 2013). One coarse ocean version, CM2.5FLORa6, has a control climate AMOC that is about 5 Sv less than that of the other, CM2.5FLOR. The models differ in their formulation of horizontal friction and mesoscale eddy parameterizations. CM2.5FLORa6 uses the same schemes as GFDL's CM2.1 model while CM2.5FLOR uses those of GFDL's ESM2M. Friction is smaller and eddy mixing is larger in the latter model (Vecchi et al 2014).

The length of integrations using eddy-resolving ocean grids is constrained by computational cost. All models have 1860 control simulations that are initialized from present day ocean initial conditions. These are run for 100 years before branching off their 1%/year CO_2 increase experiments. Because of a data transfer problem, the CM2.6 branch point was delayed until year 120. With the short spin-up, the models still have significant interior ocean temperature drift in their control experiments, although Delworth et al (2012) show that this drift is reduced in CM2.6 relative to coarse ocean climate models. The control drift is removed from all perturbation quantities presented in this study.

We also make use of 1% CO_2 increase experiments of seven additional GFDL climate models: CM2.0, CM2.1 (Delworth et al 2006), CM3 (Griffies et al, 2011), ESM2preG (Rugenstein et al 2012), ESM2G, ESM2M (Dunne et al 2012) and CM2.5 (Delworth et al. 2012). The equilibrium climate sensitivities for these models have been estimated by Stouffer et al (2006) for CM2.0 and CM2.1, Winton et al (2013b) for the ESMs and CM3, and the present study for the CM2.5 based models. The CM2.5 estimate is made using a regression of heat uptake on global temperature change in the 300-year instant CO_2 quadrupling experiments with CM2.5FLOR and CM2.5FLORa6. Twenty year means are used in the regression but the first 20 year period, containing the mixed layer adjustment (Held et al 2010), is ignored (Fig. S1). The estimate is 3.1 K, roughly in the middle of a typical multi-model range, similar to the ECSs of the other GFDL AM2-based models.

3. Results

The top panel of Figure 1 shows the global surface air temperature changes under 1%/year increasing CO_2 forcing. There are considerable differences between the simulated warming stemming from the resolution and formulation differences of the ocean components. The eddying model CM2.6 warms slightly more than CM2.5FLORa6 while CM2.5FLOR warms distinctly less than the other two models. The values for the transient climate response (TCR) – the year 61-80 average global warming – are 1.5 K for CM2.5FLOR, 1.9 K for CM2.5FLORa6, and 2.0 K for CM2.6 (Table S2). This range of TCRs spans most of a typical multi-model range. Of the 22 models compared by Winton et al (2010), 13 had TCRs in this 1.5-2.0 K range.

Figure 1 also shows the control and 1%/year CO_2 increase experiment maximum Atlantic overturning stream function at 40N for the models. There are large differences in both the control AMOC magnitudes and the magnitudes of the responses. As in previous comparisons of GFDL models (Stouffer et al 2006, Delworth et al 2012, Rugenstein et al 2013), large control climate overturning is strongly associated with a large decline under CO_2 forcing. CM2.5FLOR, which has the least surface warming, particularly in the Northern Hemisphere, has both the largest control overturning and the largest decline. CM2.5FLORa6 has the next largest control overturning and decline and CM2.6 has the smallest control AMOC and AMOC decline. The middle panel of Fig. 2 shows that the control AMOC/AMOC decline relationship in our three-model suite is consistent with that of the larger group of GFDL models. The bottom panel of Fig. 1 shows the zonal mean surface temperature change for the models. The largest differences are in the Northern Hemisphere where CM2.5FLOR has much less warming than the other two. This is an expected consequence of its larger AMOC decline (Rugenstein et al 2013). In the Southern Hemisphere, the two coarse models have less warming than the eddying model – about

0.3 K averaged over the hemisphere. Delworth et al (2012) and Bryan et al (2014) also found Southern Hemisphere warming differences between their eddying and eddy-parameterizing model. However, the eddying model had more warming in Delworth et al (2012) but less warming in Bryan et al (2014). Here we confirm the difference found by Delworth et al (2012) is associated specifically with ocean resolution and parameterizations.

The inter-model spread of Northern Hemisphere warming in our three-model suite is 0.7 K, more than double that of the Southern Hemisphere, and so we focus below on the reasons for this difference. Two aspects of the comparison displayed in Fig. 1 suggest that the differences in AMOC decline are responsible: 1) the divergence of global temperature is delayed until year 40, after the difference in the AMOCs has emerged, and 2) the main warming difference is in the Northern Hemisphere, particularly at high latitudes where Rugenstein et al (2013) and Winton et al (2013a) have demonstrated the importance of ocean circulation changes.

To allow comparison of the AMOC influence in a broader group of GFDL models with varying equilibrium sensitivities, we normalize each model's TCR by its equilibrium climate sensitivity (ECS) to form the equilibration ratio, TCR/ECS, which measures the influence of the ocean on reducing the response to radiative forcing. The top panel of Fig. 2 shows the relationship between this measure and the AMOC decline. There is a linear relationship between the three models of this study and a good correlation for the broader suite of ten GFDL models indicating an influence of the AMOC decline on the normalized warming. The middle panel of Fig. 2 shows the strong relationship between the AMOC decline under increased radiative forcing and the control climate AMOC. This relationship has been found in some other multi-model

comparisons (Gregory et al 2005; Gregory and Tailleux 2011; Weaver et al 2012) but Kostov et al (2014) find only a small correlation in their eight-model comparison of CMIP5 model responses to step CO_2 quadrupling. Gregory and Tailleux (2014) present an energy dissipation based conceptual model for the relationship. Rugenstein et al (2013) note that the control AMOC/AMOC decline relationship in some of the GFDL models is mirrored by a similar relationship between Labrador Sea convection and its response to climate change.

The bottom panel of Fig. 2 shows that there is also a strong relationship between the control AMOC and the equilibration ratio. In fact, the correlation of the equilibration ratio with the control AMOC is slightly greater in magnitude than with the AMOC decline. This might suggest that the AMOC influence on the warming is direct – through ventilation of deep water (Kostov et al 2014) – rather than indirect through the heat transport mechanism offered by Rugenstein et al (2013) and Winton et al (2013a). However, the zonal mean ocean temperature change for the experiments shown in Fig. 3 shows evidence against this interpretation. The more prominent absence of warming in the AMOC sinking region between 40N and 60N band in CM2.5FLOR indicates less heat transport into the region due to the strong AMOC decline rather than enhanced injection of the warm surface perturbation into the deep ocean by a strong control AMOC. By disallowing circulation changes in a CO_2 increase experiment, Winton et al (2013a) show that a reduction in warming in this region is associated with a circulation change as seen in the current comparison.

The AMOC/equilibration ratio relationship offers the potential for an observational constraint using AMOC observations. The Willis (2010) observation shown in Fig. 2 indicates a value for

this ratio above 0.5. However, the model AMOCs are lower at the lower latitude of the RAPID array and the observational estimate is higher (Johns et al 2012). The RAPID array measurement with its large error bar does not narrow the model range (Fig. S2). Another source of uncertainty is a difference in the relationship between simulated AMOC and Atlantic meridional heat transport compared to observations. Even when simulated AMOCs agree with observed values, the simulated heat transport is too low (Msadek et al 2013; Danabasoglu 2014). Reduced heat transport is crucial to the cooling effect of a declining AMOC (Rugenstein et al 2013; Winton et al 2013a) making a low bias in the heat transport per unit AMOC a concern for accurate simulation of the sensitivity.

The reduced surface warming in the Southern Ocean in the coarse models is seen in Fig. 3 to be associated with subsurface heat storage indicating a reduction in vertical transport of heat up to the surface in the coarse models. This feature was also found in the CM2.1/CM2.5 comparison made by Delworth et al (2012). Although Bryan et al (2014) find the opposite, that the coarse model warms more than the $1/10^{o}$ version of CCSM3.5 in the Southern Ocean, their comparison is consistent with the GFDL results in that greater surface warming is associated with less subsurface heat storage. This indicates that changes in vertical transport below the halocline are an important factor in the relative behavior of different ocean resolutions. The mechanism for these changes is unknown but might involve differences in eddy responses (Morrison et al 2013) or the mean state circulations (Marshall et al 2014a, Marshall et al 2014b).

Now we evaluate the global heat balance parameters that determine the transient climate response – the global warming at CO_2 doubling. Figure 2 shows that the models vary in their

equilibration ratios from 0.5 for CM2.5FLOR to 0.65 for CM2.6. The degree of equilibration at CO_2 doubling can be written (Winton et al 2010):

$$\frac{TCR}{ECS} = \frac{1}{1 + \varepsilon\gamma / \lambda} \qquad (1)$$

where ε is the ocean heat uptake efficacy, γ is the ocean heat uptake efficiency and λ is the equilibrium radiative feedback (= 1.13 $W/m^2/K$, the same for the three models). The ocean heat uptake efficacy is the global temperature impact of heat uptake relative to the impact of CO_2 radiative forcing, defined here as:

$$\varepsilon = \frac{\frac{ECS - TCR}{N}}{\frac{ECS}{R}} \qquad (2)$$

where N is the heat uptake and R is the radiative forcing of doubled CO_2 (assumed 3.5 W/m^2 for all models). In most models the efficacy is larger than 1 due to larger warming induced by heat uptake reductions than by CO_2 increases per Wm^{-2}. This is thought to be due to greater heat uptake occurring at higher latitudes where the climate system is more sensitive (Winton et al 2010; Armour et al 2013). Since the heat uptake efficacy and efficiency contribute to the equilibrium ratio through their product eqn. 1, we compare fractional changes in the parameters to assess their relative contributions to inter-model variations in the equilibration ratio. Variations in both efficiency and efficacy force the model equilibration spread – larger values of both are associated with lower equilibration – but the fractional variation of efficiency across the

experiments is about 3 times larger than the fractional variation of efficacy, dominating the variation of their product (Table S2).

Fig. 4 shows the inter-model relationship between ocean heat uptake efficiency and the AMOC decline and control AMOC. As in Fig. 2, the relationships within the three-model resolution suite are similar to those in the ten-model suite. Larger control AMOCs and AMOC declines are associated with larger efficiencies contributing to reduced equilibration ratio. The correlation of efficiency with control AMOC is slightly greater than its correlation with AMOC decline (similar to the equilibration ratio correlations). The correlations of the efficacy with AMOC change (-0.44) and control AMOC (0.58) were smaller than the corresponding correlations with efficiency shown in Fig. 4. Since the time-mean AMOC depends on both the control (initial) value and its change, these correlations support the connection between the time-mean AMOC strength and heat uptake parameters proposed by Kostov et al (2014). However, contrary to our finding, Kostov et al (2014) find that the AMOC decline is not correlated with their diagnosed deep ventilation parameter (see their supporting information section S3).

The causes of the increased transient climate response of MIROC3.2 hires relative to MIROC3.2 medres can also be evaluated using (1) and parameter values taken from Table 2 of Winton et al (2010). These show that the higher resolution model has a lower efficacy (0.74 vs. 0.94) and efficiency (0.60 $W/m^2/K$ vs. 0.82 $W/m^2/K$) than its medium resolution counterpart contributing to an increase in equilibration ratio from 0.50 in medres to 0.63 in hires. The GFDL and MIROC3.2 models are therefore consistent in generating greater equilibration ratio with higher ocean resolution due to reductions in both heat uptake efficiency and efficacy. Yokohata et al

(2007) also show that the coarse resolution version of MIROC3.2 has a larger control climate AMOC and AMOC decline in agreement with the GFDL model results suggesting that AMOC sensitivity differences may also contribute to the MIROC equilibration ratio differences.

4. Discussion

We have performed experiments designed to assess possible biases in the simulation of transient climate sensitivity due to the use of coarse resolution ocean components requiring eddy parameterizations. We find that the eddy parameterizations themselves significantly influence coarse model sensitivity indirectly by altering the control AMOC. The differences in transient sensitivity between the eddying and two coarse configurations of the GFDL model are associated with the magnitude of the AMOC in the control simulation. A 10-model suite of GFDL climate models, containing our 3-model subgroup, shows strong and consistent relationships between the control AMOC, its forced decline, the ocean heat uptake efficiency and the equilibration ratio (TCR/ECS). The GFDL model resolution comparison is similar to the comparison of the MIROC3.2 hires and medres models which shows that the control AMOC and AMOC decline are both reduced in the high ocean resolution model accompanying an increase in the equilibration ratio (Yokohata et al 2007).

Based on earlier work and a comparison of spatial and temporal warming patterns, we believe that the TCR differences in the GFDL model suite are mechanistically more closely related to the AMOC decline differences rather than the control AMOC differences. The reduced surface and ocean warming at high northern latitudes in CM2.5FLOR relative to the other models and the

appearance of the reduced surface warming after the AMOC decline support this connection. Rugenstein et al (2013) showed that larger AMOC decline reduces ocean heat transport to high northern latitudes counteracting the warming there. Winton et al (2013a) showed that fixing ocean circulation (including AMOC) in a CO_2 increase experiment substantially increased warming in the GFDL ESM2M model, particularly at high latitudes. However, Kostov et al (2014) find that the control AMOC is more closely related to surface climate change in their comparison of CMIP5 model responses to instant CO_2 quadrupling. It is not clear whether this difference from our study arises from differences in the forcings, models used, or analysis techniques. The common finding of both studies, that there is a relationship between the transient warming and the control AMOC is encouraging in that it may allow application of observational constraints.

In addition to the GFDL models compared here, other high resolution climate models have produced weaker AMOCs than their lower resolution counterparts (Junclaus et al 2013; Delworth et al 2012; Sakamoto et al 2012; Shaffrey et al 2009; Yokohata et al 2007). This may be due to the widening of North Atlantic straits in order to represent their depths in the lower resolution models. As the strait width becomes resolved, the influence of dense-water outflows diminishes. The additional resolution, horizontal and vertical, needed to maintain these outflows as they proceed downslope has not been attained even in the high resolution models (Winton et al 1998). If this is the cause of the AMOC reduction in eddying models, a high bias in transient climate sensitivity may have been introduced into the *high* resolution models. The AMOC is an emergent property of the climate simulation, however, and is subject to many other atmospheric and oceanic influences that temper the direct influence of resolution.

Even if the global sensitivities of our coarse and eddying models can be reconciled by accounting for AMOC differences, a difference in the distribution of the warming remains with the Southern Ocean warming relatively more in the eddying model. Bryan et al (2014) found the opposite Southern Ocean warming sensitivity with the NCAR CCSM3.5 suggesting that this difference does not have a robust association with resolution. Rather we find that that the vertical pattern of warming indicates that the decline in Southern Ocean vertical transport induced by climate change is sensitive to resolution but the sense of this sensitivity is uncertain.

To summarize, there is no clear indication of an inherent transient sensitivity bias due to coarse ocean resolution in the few tests that have been done to date. However more study of the role of resolution in the simulation of the AMOC and Southern Ocean transport is needed to build confidence in this conclusion.

Acknowledgements

The authors thank Kyle Armour, Isaac Held, Yavor Kostov, John Marshall, Rong Zhang, and two anonymous reviewers for comments on the manuscript. Comprehensive model output for the GFDL CM2.0, CM2.1, CM3, ESM2M and ESM2G models is available from the CMIP archives. The cited summary statistics for all models are available from the first author.

References

Armour, Kyle C., Cecilia M. Bitz, Gerard H. Roe, 2013: Time-Varying Climate Sensitivity from Regional Feedbacks. J. Climate, 26, 4518–4534.doi: http://dx.doi.org/10.1175/JCLI-D-12-00544.1

Bryan, F.O., P.R. Gent, R. Tomas, 2014: Can Southern Ocean Eddy Effects Be Parameterized in Climate Models? J. Climate, 27, 411–425.

Danabasoglu, G., and coauthors, 2014: North Atlantic simulations in Coordinated Ocean-ice Reference Experiments phase II (CORE-II). Part I: Mean states, Ocean Modeling, 73, 76—107.

Delworth, T.L., and Coauthors, 2012: Simulated Climate and Climate Change in the GFDL CM2.5 High-Resolution Coupled Climate Model. J. Climate, 25, 2755–2781.

Delworth, Thomas L., and Coauthors, 2006: GFDL's CM2 global coupled climate models. Part I: formulation and simulation characteristics. J. Climate, 19, 643–674. doi: http://dx.doi.org/10.1175/JCLI3629.1

Dunne, J.P., J. John, A. Adcroft, S.M. Griffies, R.W. Hallberg, E. Shevliakova, R.J. Stouffer, W.F. Cooke, K.A. Dunne, M.J. Harrison, J.P. Krasting, S. Malyshev, P.C.D. Milly, P. Phillipps, L.T. Sentman, B.L. Samuels, M.J. Spelman, M. Winton, A.T. Wittenberg, and N. Zadeh, 2012: GFDL's ESM2 global coupled climate-carbon Earth System Models Part I: Physical formulation

and baseline simulation characteristics. Journal of Climate, 25(19), DOI:10.1175/JCLI-D-11-00560.1.

Gent, P. R. and J. C. McWilliams, 1990: Isopycnal mixing in ocean general circulation models. Journal of Physical Oceanography, 20, 150–155.

Gregory, J.M., and R. Tailleux, 2011: Kinetic energy analysis of the response of the Atlantic meridional overturning circulation to CO2-forced climate change, Climate Dynamics, 37:893–914. DOI 10.1007/s00382-010-0847-6

Gregory, J. M., and coauthors, 2005: A model intercomparison of changes in the Atlantic thermohaline circulation in response to increasing atmospheric CO2 concentration, Geophys. Res. Lett., 32, L12703, doi:10.1029/ 2005GL023209.

Griffies, S.M., M. Winton, L.J. Donner, L.W. Horowitz, S.M. Downes, R. Farneti, A. Gnanadesikan, W.J. Hurlin, H-C. Lee, Z. Liang, J.B. Palter, B.L. Samuels, A.T. Wittenberg, B. Wyman, J. Yin, and N. Zadeh, 2011: The GFDL CM3 Coupled Climate Model: Characteristics of the ocean and sea ice simulations. Journal of Climate, 24(13), doi:10.1175/2011JCLI3964.1.

Held, I.M., M. Winton, K. Takahashi, T.L. Delworth, F. Zeng, and G.K. Vallis, 2010: Probing the fast and slow components of global warming by returning abruptly to pre-industrial forcing. Journal of Climate, 23(9), doi:10.1175/2009JCLI3466.1.

Johns, W. E., and Coauthors, 2011: Continuous, Array-Based Estimates of Atlantic Ocean Heat Transport at 26.5°N. J. Climate, 24, 2429–2449. doi: http://dx.doi.org/10.1175/2010JCLI3997.1

Jungclaus, J. H., N. Fischer, H. Haak, K. Lohmann, J. Marotzke, D. Matei, U. Mikolajewicz, D. Notz, and J. S. vonStorch, 2013: Characteristics of the ocean simulations in MPIOM, the ocean component of the MPI-Earth system model, J. Adv. Model. Earth Syst., 5, 422–446, doi:10.1002/jame.20023.

Kirtman, B.P., and Coauthors, 2012: Impact of ocean model resolution on CCSM climate simulations. Climate Dynamics, 39, 1303-1328, DOI: 10.1007/s00382-012-1500-3.

Kostov, Y., K. C. Armour, and J. Marshall (2014), Impact of the Atlantic meridional overturning circulation on ocean heat storage and transient climate change, Geophys. Res. Lett., 41, 2108–2116, doi:10.1002/2013GL058998.

Kuhlbrodt, T., and J. M. Gregory 2012: Ocean heat uptake and its consequences for the magnitude of sea level rise and climate change, Geophys. Res. Lett., 39, L18608, doi:10.1029/2012GL052952.

Marshall, J., Armour, K., Scott, J., Kostov, Y., Hausmann, U., Ferreira, D., Shepherd, T., and Bitz, C., 2014a: The ocean's role in polar climate change: asymmetric Arctic and Antarctic responses to greenhouse gas and ozone forcing, Philosophical Transactions of the Royal Society A: Mathematical, Physical and Engineering Sciences, vol. 372, no. 2019.

Marshall, J., Scott, J.R., Armour, K.C., Campin, J-M., Kelley, M., and Romanou, A., 2014b: The ocean's role in the transient response of climate to abrupt greenhouse gas forcing, Climate Dynamics, doi:10.1007/s00382-014-2308-0.

McClean, J.L., D.C. Bader, F.O. Bryan, M.E. Maltrud, J.M. Dennis, A.A. Mirin, P.W. Jones, Y.Y. Kim, D.P. Ivanova, M, Vertenstein, J.S. Boyle, R.L. Jacobs, N. Norton, A. Craig, and P.H. Worley, 2011: A prototype two-decade fully-coupled fine resolution CCSM simulation. Ocean Modelling, doi:10.1016/jocemod.2011.02.011.

Morrison, A. K., O. A. Saenko, A. M. Hogg, and P. Spence, 2013: The role of vertical eddy flux in Southern Ocean heat uptake. Geophysical Research Letters, 40 (20), 5445–5450.

Msadek, Rym, William E. Johns, Stephen G. Yeager, Gokhan Danabasoglu, Thomas L. Delworth, Anthony Rosati, 2013: The Atlantic Meridional Heat Transport at 26.5°N and Its Relationship with the MOC in the RAPID Array and the GFDL and NCAR Coupled Models. J. Climate, 26, 4335–4356.

Palter JB, Griffies SM, Galbraith ED, Gnanadesikan A. Samuels B, Klocker A., 2013: The driving processes of the deep ocean buoyancy budget and their temporal variability. doi: 10.1175/JCLI-D-13-00016.1

Rugenstein, M, M. Winton, R.J. Stouffer, S.M. Griffies, and R.W. Hallberg, 2013: Northern high latitude heat budget decomposition and transient warming. J. Climate, 26(2), DOI:10.1175/JCLI-D-11-00695.1.

Sakamoto, T.T., and coauthors, 2012: MIROC4h – A new high-resolution atmosphere-ocean coupled general circulation model, Journal of the Meteorological Society of Japan, 90(3), 325—359.

Shaffrey, L. C., and Coauthors, 2009: U.K. HiGEM: The New U.K. High-Resolution Global Environment Model—Model Description and Basic Evaluation. J. Climate, 22, 1861–1896.

Stouffer, R. J., and Coauthors, 2006: GFDL's CM2 Global Coupled Climate Models. Part IV: Idealized Climate Response. J. Climate, 19, 723–740.
doi: http://dx.doi.org/10.1175/JCLI3632.1

Vecchi, G.A., T. Delworth, R. Gudgel, S. Kapnick, A. Rosati, A.T. Wittenberg, F. Zeng, W. Anderson, V. Balaji, K. Dixon, L. Jia, H.-S. Kim, L. Krishnamurthy, R. Msadek, W.F. Stern, S.D. Underwood, G. Villarini, X. Yang, S. Zhang, 2014: On the Seasonal Forecasting of Regional Tropical Cyclone Activity, J. Climate, in press. http://dx.doi.org/10.1175/JCLI-D-14-00158.1

Weaver, A. J., and Coauthors, 2012: Stability of the Atlantic meridional overturning circulation: A model intercomparison, Geophys. Res. Lett., 39, L20709, doi:10.1029/2012GL053763

Willis, J. K., 2010: Can in situ floats and satellite altimeters detect long-term changes in Atlantic Ocean overturning? Geophys. Res. Lett., 37, L06602, doi:10.1029/2010GL042372.

Winton, M., S.M. Griffies, B.L. Samuels, J.L. Sarmiento, T.L. Frölicher, 2013a: Connecting Changing Ocean Circulation with Changing Climate. J. Climate, 26, 2268–2278.

Winton, M., A. Adcroft, S.M. Griffies, R.W. Hallberg, L.W. Horowitz, and R.J. Stouffer, 2013b: Influence of ocean and atmosphere components on simulated climate sensitivities. Journal of Climate, 26(1), DOI:10.1175/JCLI-D-12-00121.1.

Winton, M., K. Takahashi, and I.M. Held, 2010: Importance of ocean heat uptake efficacy to transient climate change. Journal of Climate, 23(9), doi:10.1175/2009JCLI3139.1.

Winton, M., R.W. Hallberg, and A. Gnanadesikan, 1998: Simulation of density-driven frictional downslope flow in z-coordinate ocean models. J. Phys. Oceanogr., 28(11).

Yokohata, T., et al., 2007: Different transient climate responses of two versions of an atmosphere-ocean coupled general circulation model, Geophys. Res. Lett., 34, L02707, doi:10.1029/2006GL027966.

List of Figures

Figure 1. Top: global mean surface temperature changes in 1%/year CO_2 increase experiments (TCR 95% CI's shown at right). Middle: maxima of meridional overturning stream functions at 40N in the Atlantic in control (dotted) and 1%/year CO_2 increase (solid). Bottom: zonal mean surface air temperature changes at CO_2 doubling (year 61-80 average) in 1%/year CO_2 increase experiments.

Figure 2. GFDL climate model relationships between the equilibration ratio (TCR/ECS) and the AMOC decline (top), between the control climate AMOC and the AMOC decline (middle), and between the control climate AMOC and the equilibration ratio (bottom). Red dashed lines fit the relationships for the 3-model subgroup and the black dashed lines fit the 10-model suite relationships.

Figure 3. Zonal mean ocean temperature change at CO_2 doubling (year 61-80 average) in 1%/year CO_2 increase experiments: CM2.6 (top), CM2.5FLORa6 (middle), and CM2.5FLOR (bottom).

Figure 4. GFDL climate model relationships between AMOC decline and ocean heat uptake efficiency (top) and between control AMOC and efficiency (bottom). Red dashed lines fit the relationships for the 3-model subgroup and the black dashed lines fit the 10-model suite relationships.

Figure 1. Top: global mean surface temperature changes in 1%/year CO_2 increase experiments (TCR 95% CI's shown at right). Middle: maxima of meridional overturning stream functions at 40N in the Atlantic in control (dotted) and 1%/year CO_2 increase (solid). Bottom: zonal mean surface air temperature changes at CO_2 doubling (year 61-80 average) in 1%/year CO_2 increase experiments.

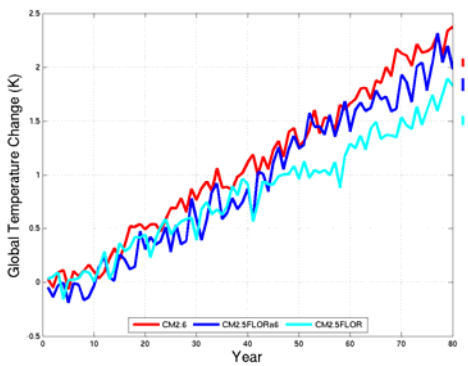

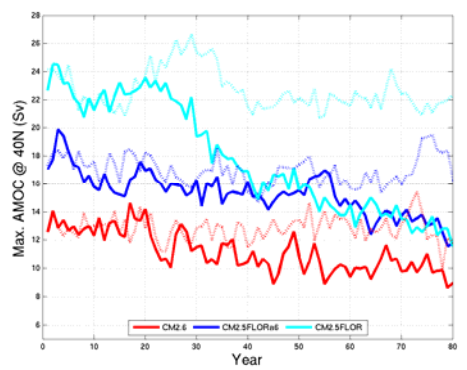

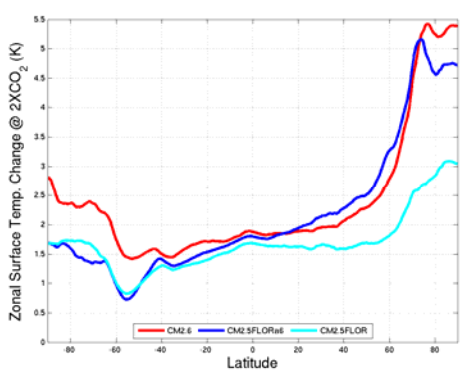

Figure 2. GFDL climate model relationships between the equilibration ratio (TCR/ECS) and the AMOC decline (top), between the control climate AMOC and the AMOC decline (middle), and between the control climate AMOC and the equilibration ratio (bottom). Red dashed lines fit the relationships for the 3-model subgroup and the black dashed lines fit the 10-model suite relationships.

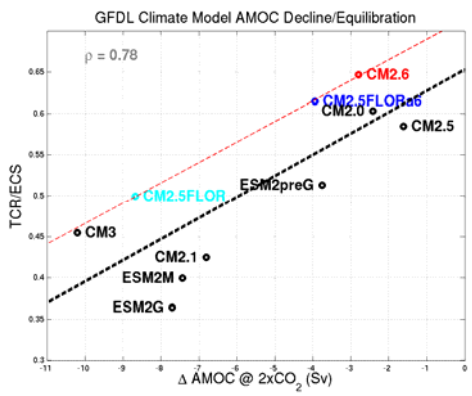

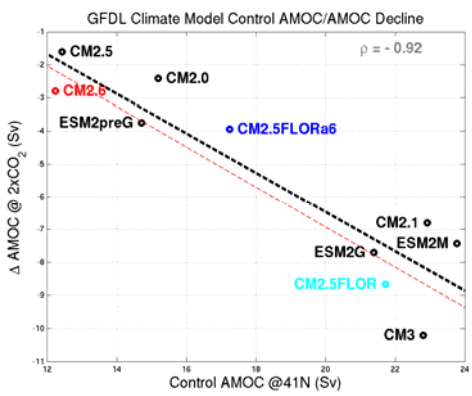

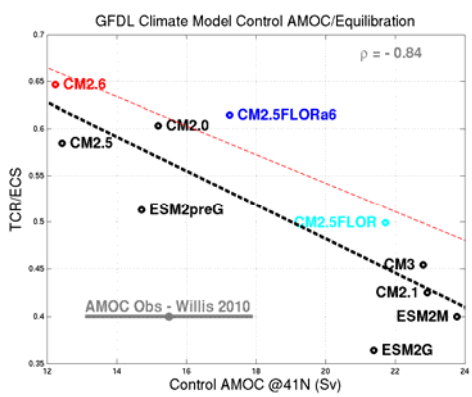

Figure 3. Zonal mean ocean temperature change at CO_2 doubling (year 61-80 average) in 1%/year CO_2 increase experiments: CM2.6 (top), CM2.5FLORa6 (middle), and CM2.5FLOR (bottom).

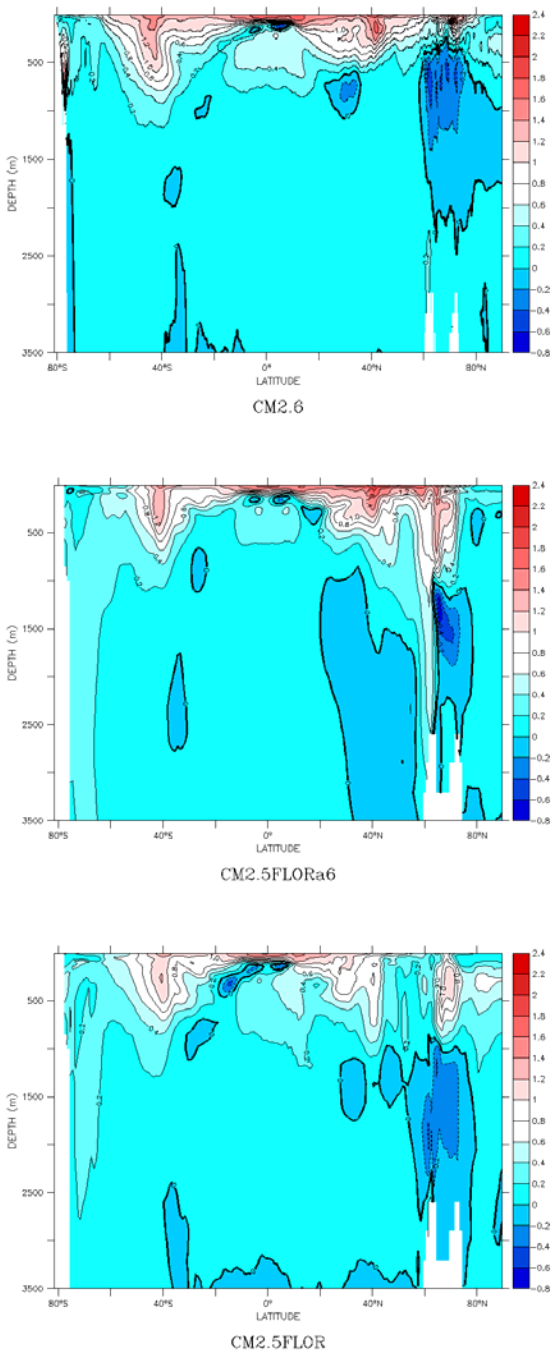
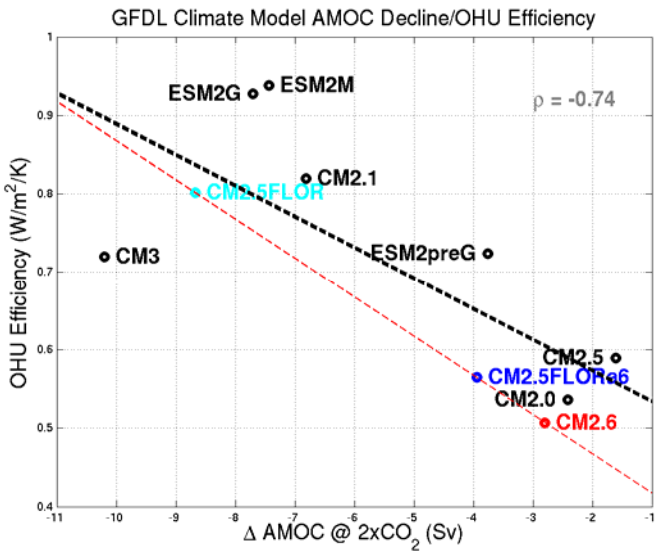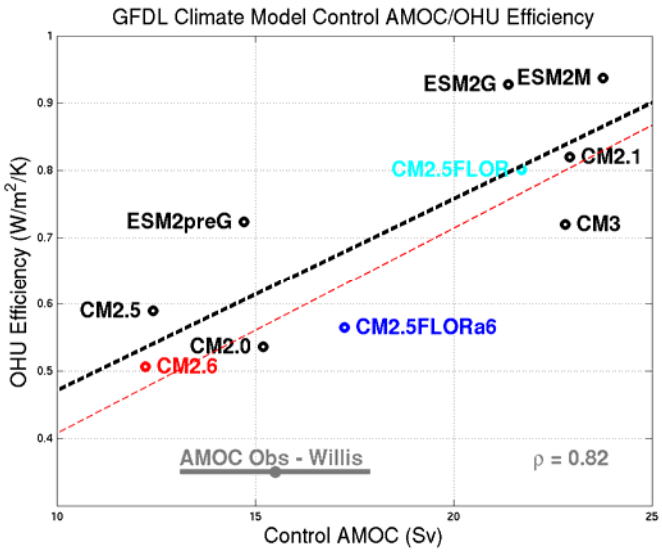
Figure 4. GFDL climate model relationships between AMOC decline and ocean heat uptake efficiency (top) and between control AMOC and efficiency (bottom). Red dashed lines fit the relationships for the 3-model subgroup and the black dashed lines fit the 10-model suite relationships.